Original Article

OPEN

Histological evidence supporting the durability of successful radiofrequency renal denervation in a normotensive porcine model

Andrew S.P. Sharp[a], Stefan Tunev[b], Markus Schlaich[c], David P. Lee[d], Aloke V. Finn[e], Julie Trudel[b], Douglas A. Hettrick[b], Felix Mahfoud[f], and David E. Kandzari[g]

Background: Sustained blood pressure reductions after radiofrequency (RF) renal denervation (RDN) have been reported to 3 years in patients with uncontrolled hypertension. However, mechanistic data to support procedural durability are lacking. We aimed to quantify the long-term nerve anatomic and functional effects of RF RDN in a preclinical model.

Methods: Bilateral RF RDN was performed in 20 normotensive swine. Renal tissue samples were obtained in the RDN-treated groups at 7 ($n = 6$), 28 ($n = 6$), and 180 days ($n = 8$) postprocedure for quantification of cortical norepinephrine (NE) levels and renal cortical axon density. Tissue fibrosis, necrosis and downstream nerve fiber atrophy (axonal loss) were also scored for each sample. Three additional untreated groups ($n = 6$, $n = 6$ and $n = 8$, respectively) served as control.

Results: Pathologic nerve changes were characterized by necrosis in the ablated region at 7 days that partially resolved by 28 days and fully resolved at 180 days. Axonal loss was apparent within and downstream to the ablation regions and was evident at 7, 28 and 180 days in the main vessel and branch vessels. Consequently, renal cortical axon density and corresponding cortical NE levels were significantly reduced at 7 days in the RDN vs. control group and remained suppressed at 180 days.

Conclusions: Reductions in renal NE, cortical axon density and downstream axonal loss caused by axonal destruction persisted through 180 days post-RDN in a normotensive swine model. These results suggest functional nerve regrowth after RF RDN is unlikely and support published clinical evidence that the procedure results in durable blood pressure reduction.

Keywords: nerve regeneration, radiofrequency, renal denervation, Schwann cells, sympathetic nervous system

Abbreviations: BP, blood pressure; NE, norepinephrine; RDN, renal denervation; RF, radiofrequency

INTRODUCTION

Hypertension remains the leading treatable global cause of mortality due to the unique combination of high adult incidence, poor rates of control despite the availability of safe and effective drug therapy, and strong association with target organ damage [1]. Thus, adjunctive nonpharmacologic hypertension treatment options are desirable.

The safety and efficacy of catheter-based renal denervation (RDN) for blood pressure (BP) reduction has recently been demonstrated in several randomized, sham-controlled trials using radiofrequency (RF) [2,3] and ultrasound [4,5] energy-based systems in both the presence and absence of concomitantly prescribed antihypertensive drug therapy. Long-term durability of blood pressure reduction following RF RDN has also been demonstrated by all-comer registries [6,7] including the Global SYMPLICITY registry, which has demonstrated significant BP reductions to 3 years in over 2500 patients without an increase in prescribed antihypertensive medications [6,8]. However, pathological data to support the anatomical durability of an initially effective ablation procedure are limited.

The RDN procedure is associated with reductions in markers of sympathetic activity including muscle sympathetic nerve activity [9,10] and renal norepinephrine spillover in humans [11]. Unfortunately, no practically useful clinical test is currently available to confirm anatomical and functional nerve ablation, nor to demonstrate absence of reinnervation in human individuals. Prior animal models have raised the possibility of anatomical and functional reinnervation [12–17], although other models have demonstrated sustained BP reduction following RDN [14,16]. Absence of myelination in renal sympathetic nerves exposes the renal axon body more directly to RF energy and may also limit the possibility of functional regrowth of

renal nerves following initial axonal destruction [15]. We characterized the pathophysiological processes associated with the durability of nerve destruction in a normotensive porcine model.

METHODS

Study design

Studies were performed in accordance with the Guide for the Care and Use of Laboratory Animals of the National Institutes of Health (Publication Number 85-23, revised 1996), in compliance with the Animal Welfare Act and the U.S. Food and Drug Administration regulations and their amendments.

Yorkshire domestic farm swine ($N = 20$) of either sex, weighing between 35 and 50 kg, were assigned to three groups for histological study at 7 days (group 1, $n = 6$), 28 days (group 2; $n = 6$) and 180 days (group 3, $n = 8$) post procedure (Fig. 1). Three separate groups of surgically untreated animals ($n = 6$, $n = 6$, and $n = 8$, respectively) underwent identical tissue analysis and served as controls. Within each study group and during general anesthesia with isoflurane following induction with xylazine and propofol, a 6F or 7F introducer sheath was positioned in the ostium of the renal artery by percutaneous cannulation of the right femoral artery under fluoroscopic guidance. The multielectrode radiofrequency RDN catheter (Spyral; Medtronic, Santa Rosa, CA, USA) was advanced over a 0.014 guide wire sequentially into the right and left renal artery as previously described [18,19]. The guide wire was partially withdrawn following catheter positioning to allow the device to achieve its natural helical shape in opposition to the vessel wall. Two 60-s RF energy applications were delivered simultaneously in each main renal artery via the four catheter electrodes (up to eight lesions). Additional denervation was performed in the primary branch vessels (one cycle of up to four lesions) in the 180-day group following the modifications made to the clinical procedure in light of increased understanding of the sympathetic nervous system anatomy [20] to demonstrate durability of the current clinical procedural approach.

Animals were humanely sacrificed via pentabarbital overdose according to grouping and serial histological tissue samples of the kidney renal arteries and surrounding tissues were obtained in each group at 7, 28, and 180 days postprocedure, respectively, as previously described [18]. Briefly, the renal arterial tree was sectioned every 3–4 mm along the longitudinal access of the artery including treated and untreated regions, and each resulting sample was stained with hematoxylin and eosin. Necrosis was identified by obliteration of nerve structure, presence of nerve cell debris, hypercellularity, loss of blood vessels and transformation to phagocytic Schwann cell phenotype. Fibrosis was characterized by disruption of normal nerve structure, visible fibrosis and hypercellularity. Neuromatous regeneration was identified by sprouting of small nerve radicles in the perineurium and around damaged nerves. Tissue necrosis, fibrosis, nerve body atrophy (axonal loss) and neuromatous regeneration were each blindly assessed via an established semi quantitative scale of 0–3 including both ablated and nonablated regions, (0 = no change/normal features; 1 = present, but minimal feature; 2 = notable feature not effacing preexisting tissue elements or limited to a small tissue area; 3 = overwhelming feature involving large tissue areas) [21]. Renal sympathetic nerve variability was further assessed by quantitative immunohistochemistry to determine the density of terminal axons in the renal cortex. Embedded tissue samples from each kidney were stained immunohistochemically for tyrosine hydroxylase as an indicator of viable sympathetic nerves. The cross sectional area and number of intact (tyrosine hydroxylase positive) renal nerves was assessed via automated digital morphometry and the terminal sympathetic axons were quantified in the renal cortex as a density of positively stained events in the observed sections normalized to observed area. Finally, renal norepinephrine (NE) content was determined on treated and untreated kidneys via using high-performance liquid chromatography.

Statistical analysis

Since RDN was performed bilaterally, each animal contributed two kidneys for analysis. All reported values are expressed as mean ± standard deviation (SD) calculated from the raw data. Normalized differences between the control and treatment groups were calculated and are reported for convenience of relative comparison; however, all statistical analyses were performed on non-normalized values. Differences in renal NE concentration and axonal density were evaluated using unpaired Student t tests with Welch's correction. P values for all comparisons were two-sided, and values obtained from different tissues of the same animal were considered independent for statistical purposes.

RESULTS

Renal denervation was successfully performed in all animals in the RDN groups. Photographic examples of pathologic nerve changes observed are shown in Figs. 2–3. Viable functioning renal nerves, as identified by tyrosine hydroxylase staining, were apparent in the untreated groups (Fig. 4). However, renal cortical axon density and
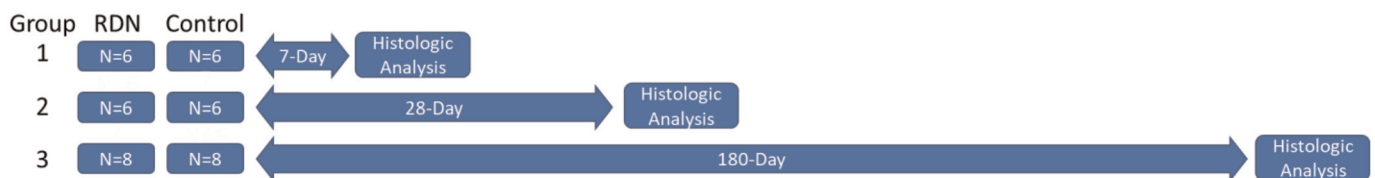

FIGURE 1 Diagram of experimental design. Tissue samples were obtained and analyzed from healthy swine at 7, 28 and 180 days post radiofrequency renal denervation. Identical groups of untreated animals served as controls.
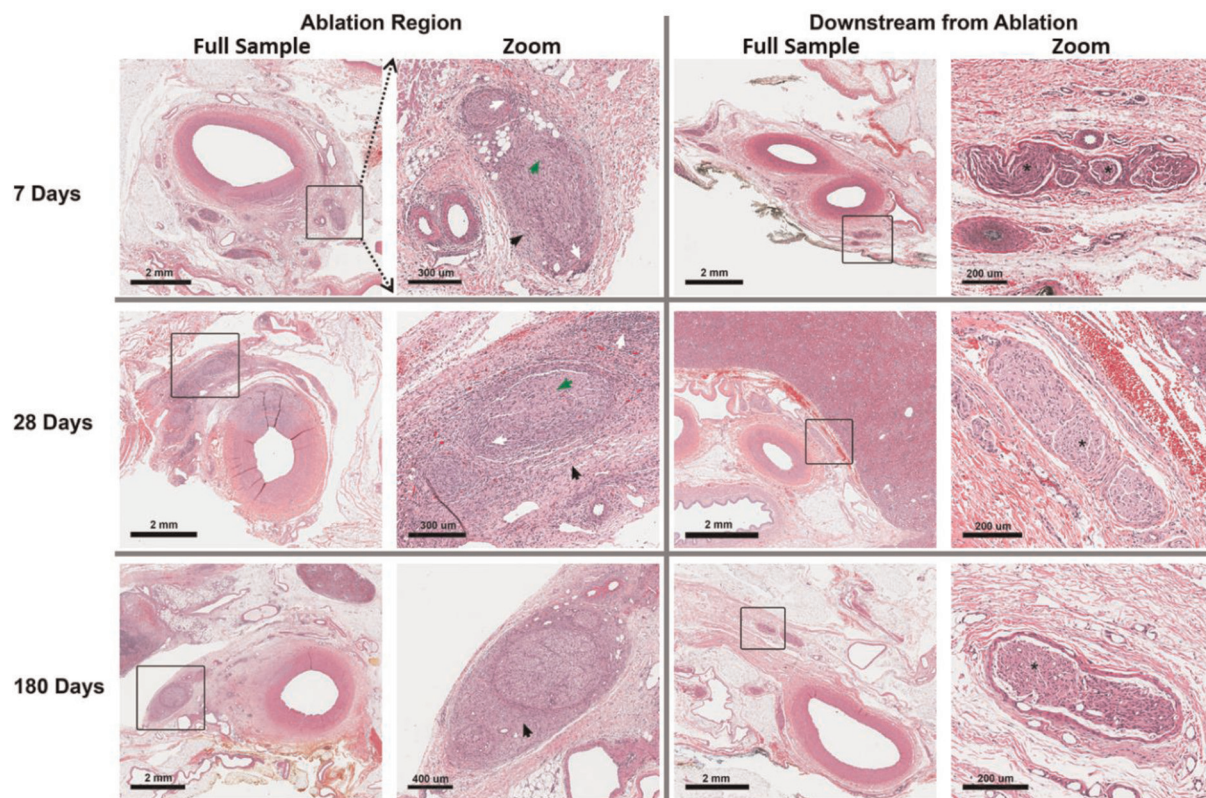
FIGURE 2 Examples of changes in nerve histology pos-tablation. Changes in nerve histology in the ablation region (left) and downstream from the ablation region (right) are shown in full sample view as well as zoomed-in view (black square area). At 7 days post radiofrequency renal denervation, inflammation (white arrow head examples), fibrosis (black arrow) and necrosis (green) are apparent in the ablated region. At 180 days, necrosis was no longer evident but fibrosis remained in the ablated region. Axonal loss (destruction of axonal body) was present within and downstream (∗) to the ablated regions at all timepoints.
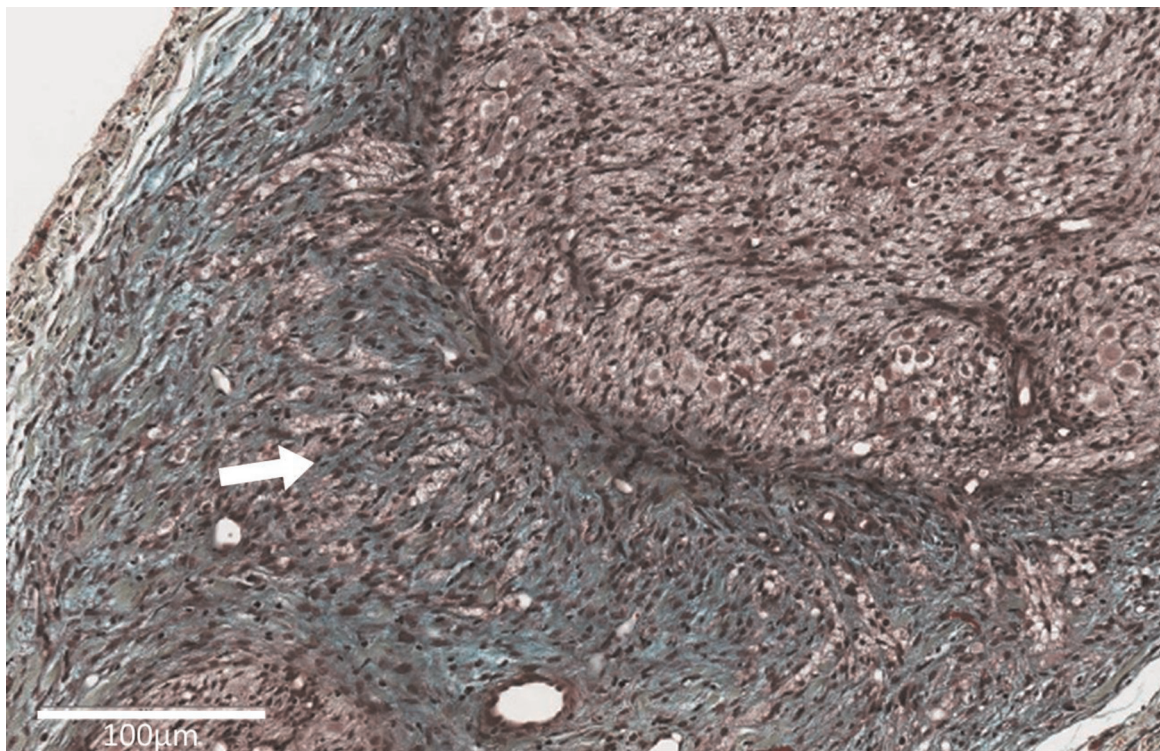

FIGURE 3 Schwann Cell proliferation and fibrosis. Chaotic extra-neuronal Schwann cell proliferation (arrow) and fibrotic response at the site of RF treatment at 180 days. Anatomic proliferation was not associated with downstream functional axonal connections. Brown staining indicates Schwann cells. Green staining indicates fibrosis.
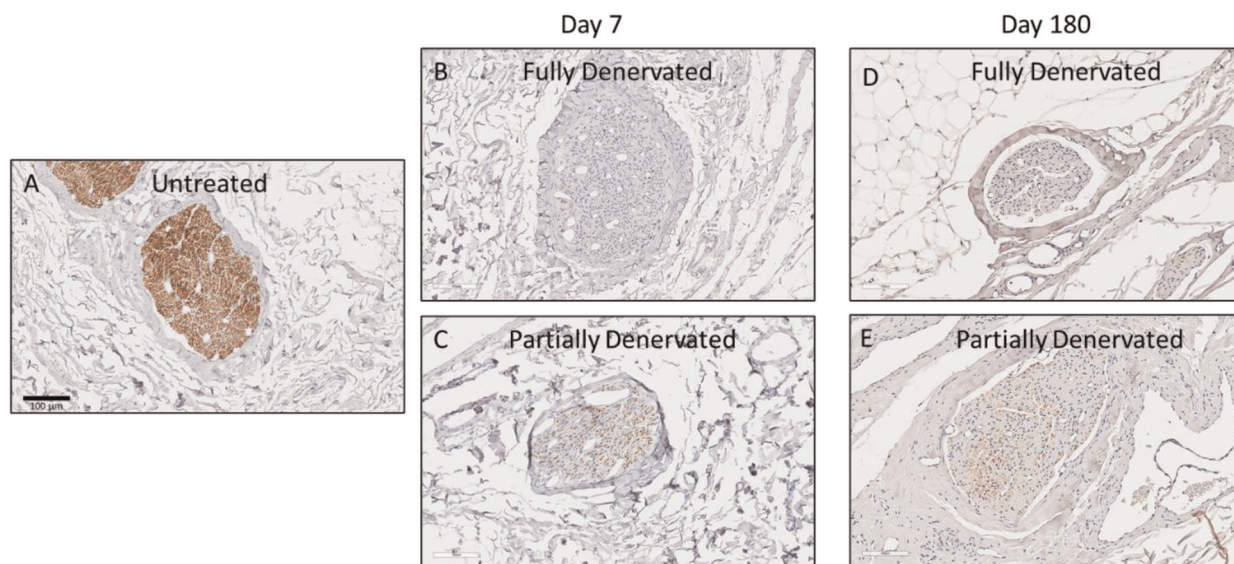
FIGURE 4 Tyrosine hydroxylase renal nerve staining. Examples of tyrosine hydroxylase nerve staining of untreated (a), full treated (b,d) and partially denervated (c,e) nerve bundles. Fully denervated nerve bundles do not stain due to absence of neuronal axons at both 7 and 180 days post denervation. Partially denervated nerves, also present at both 7 and 180 days, did not regenerate new axonal connections but remained partially denervated at 180 days.

corresponding cortical norepinephrine levels were significantly reduced in the RDN versus control group at 7 days and remained suppressed through 28 and 180 days (Fig. 5). Nerve necrosis was apparent primarily in the ablated region at 7 days (average score: 1.02 ± 0.26), but decreased in magnitude at 28 days (0.13 ± 0.19) and was not detectable in any sample at 180 days as the inflammatory response receded (Fig. 6a−c). Subsequent nerve fibrosis was confined to the ablated regions (Fig. 6d−f) and was consistent at 7 days (0.76 ± 0.39), 28 days (1.00 ± 0.35) and 180 days (1.20 ± 0.30). Axonal loss was apparent both within the ablation regions and downstream (Fig. 6g−i) and was evident in the main renal artery at 7 days (0.76 ± 0.39) and 28 days (0.60 ± 0.28) and in both the main and branch vessels at 180 days (0.70 ± 0.60). Chaotic extra-neuronal Schwann cell proliferation occurred around the site of RF treatment, but this was not associated with downstream functional axonal connections (Figs. 3 and 7). Neuromatous regeneration was not apparent in any sample at 7 days. Nerve regeneration score at 28 days (0.24 ± 0.25) was similar to 180 days (0.20 ± 0.10) with distribution mostly confined to region of ablation. Neuromatous regeneration scored indices were significantly different than control group ($P < 0.001$).

DISCUSSION

Unlike central nerves, postganglionic renal sympathetic nerves are nonmyelinated. This difference is important since the lack of myelination leaves no clear structural framework for reinnervation to occur following ablation. In this prospective study, histological analysis of renal tissue post radiofrequency denervation demonstrated transient nerve necrosis followed by persistent fibrosis of renal nerves at the ablation site. These findings were associated with downstream axonal destruction and atrophic nerve body changes, suggesting irreparable damage of nerve

architecture with mature fibrotic infiltration at 180 days. Residual Schwann cells produced chaotic nonmyelinated nerve tissue consistent with focal nonfunctional neuromatous regeneration around the ablation site. These anatomical findings imply that long-term recurrence of functional axonal connections distal to the treated site is unlikely. Consistent with these anatomic observations, renal norepinephrine content and corresponding renal cortical axon density were persistently reduced at 7, 28 and 180 days in the RDN compared with control groups.

The hypothesis that renal nerves will regenerate and yield only temporary benefits of RDN has not been supported by clinical experience in humans, despite mixed reports from prior animal work. Functional efferent and afferent reinnervation of the renal vasculature has been demonstrated within weeks after surgical RDN in normal rats [12,17,22]. However, such morphological evidence of sympathetic regrowth was not accompanied by recovery in renal NE content [23]. Another recent study showed anatomical evidence of renal sympathetic and sensory nerve regrowth 4 weeks post procedure in hypertensive rats, but with sustained BP reduction relative to sham animals [16]. Likewise, both anatomical and functional re-innervation were demonstrated 11 months after RF RDN in normotensive sheep via histological staining and response to stimulation, respectively [13]. However, the same group subsequently reported results from an ovine model of chronic kidney disease showing sustained reductions in BP with cardio- and reno-protection 30 months following RF RDN, despite partial functional recovery [14]. Lack of functional recovery was also reported based on sustained natriuresis and suppressed renin release one year after surgical denervation in dogs [24]. Furthermore, a model comparable to the present analysis in healthy swine identified neuromatous tangles with disorganized architecture and distal axonal loss at 90 days following RDN with RF energy making potential functional regenerative activity
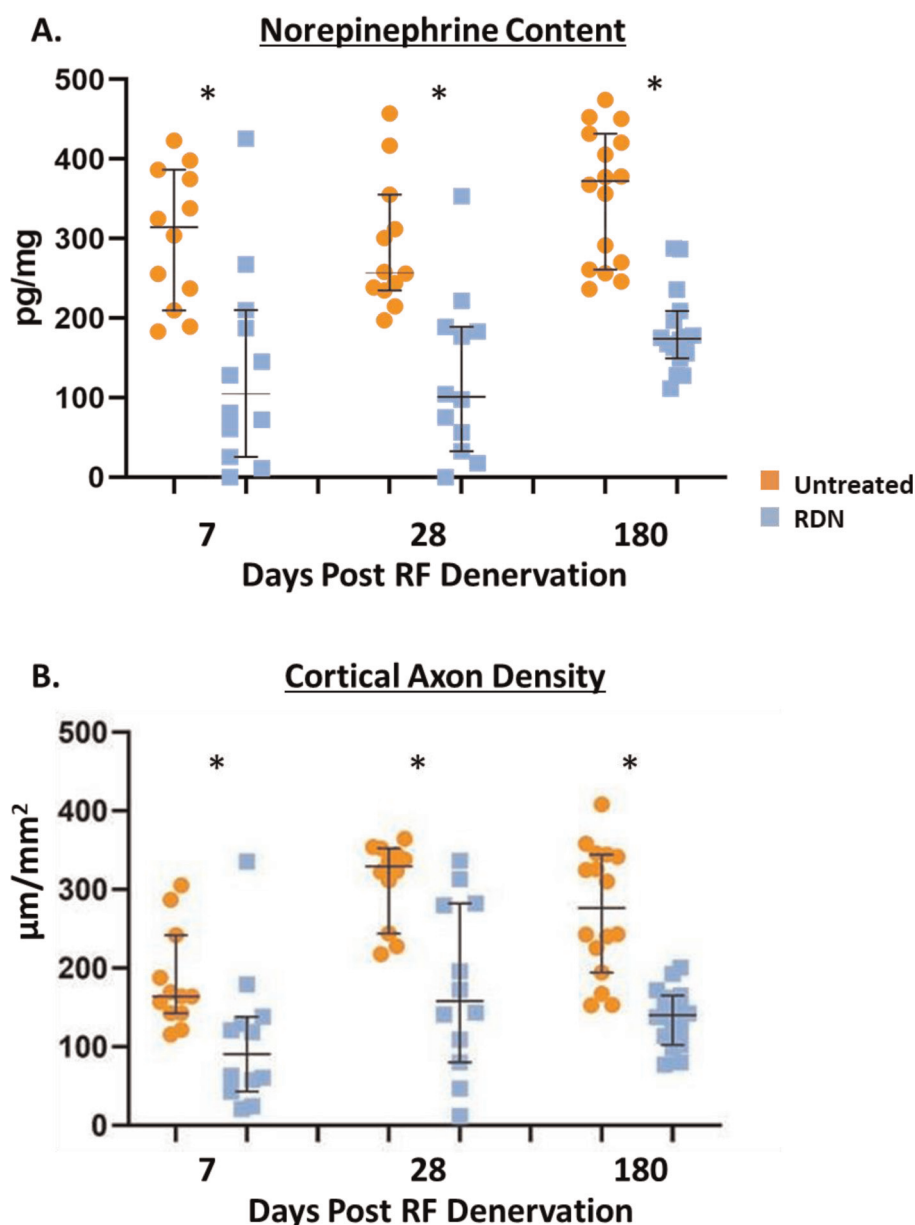
A. Norepinephrine Content

B. Cortical Axon Density

FIGURE 5 Changes in renal norepinephrine content and cortical axon density. Comparison of changes in renal norepinephrine content (a) and renal cortical axon density (b) between radiofrequency renal denervation at 7, 28 and 180 days post radiofrequency renal denervation with untreated control groups. Both norepinephrine and renal cortical axon density were lower compared to control at all time points. Each animal contributed 2 kidneys for analysis. $*P < 0.001$ for all between group comparisons.

unlikely [15]. Data supporting functional nerve generation following renal transplant in humans are also mixed. Despite some histological evidence for regeneration of renal nerve fibers within a year following transplant [25,26], other analysis has shown no evidence of functional efferent reinnervation after 2 months and 2 years [27]. Hence, anatomic re-innervation does not necessarily imply functional re-innervation. Taken within the context of the present results, apparent functional recovery in animal models could alternatively be explained by hyperfunctionality of residual undamaged or partially damaged nerves [28]. Indeed, we observed that partially damaged nerves with identical morphologies were present at all follow up durations, indicating that incomplete ablation of these nerves

remains stable, yet new functional axons do not appear. Our results could also be extrapolated to imply that so called RDN 'nonresponders', defined as patients with minimal or no BP reduction following the procedure, are not necessarily the result of nerve regrowth, but could result from any of a number of factors such as decreased antihypertensive drug adherence, nonsympathetically mediated hypertension etiology, or incomplete ablation.

Recent anatomical analysis of human cadavers identified complex fused combinations of the aorticorenal, celiac, and superior mesenteric ganglia near the renal artery ostium [20,29]. The renal nerve bundles surrounding the renal artery do not form a typical renal nerve plexus, especially near the ostium. These ganglia are associated
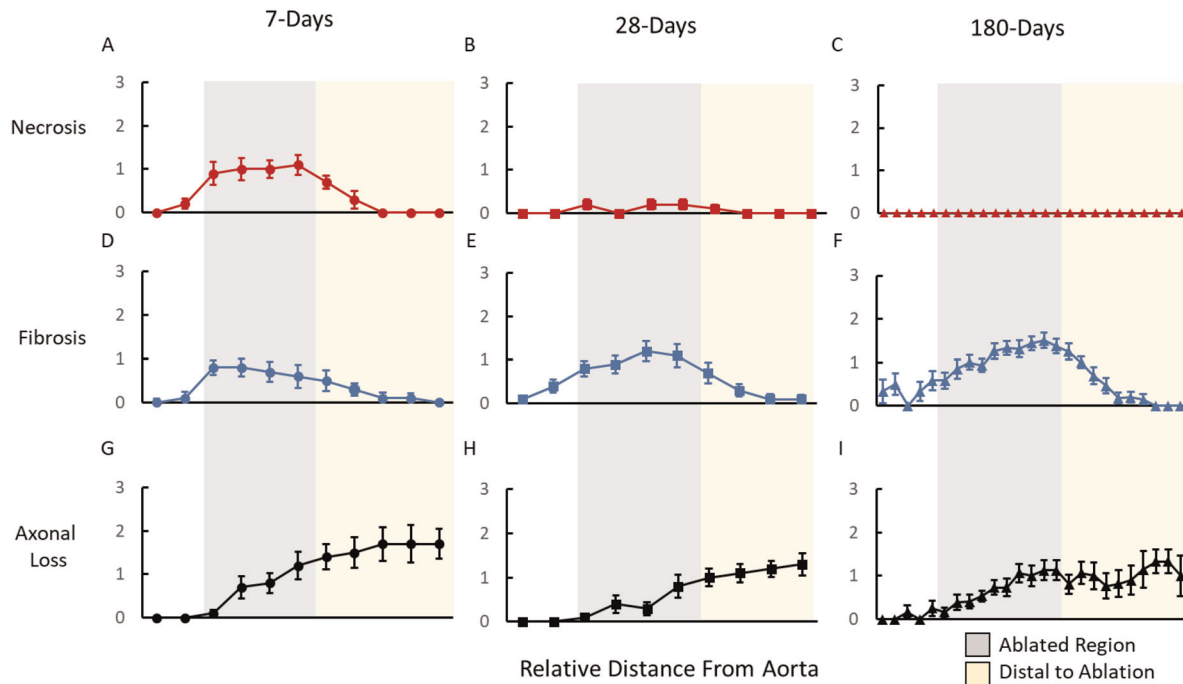
FIGURE 6 Quantification of mean tissue necrosis, fibrosis and nerve body atrophy. Quantification of mean tissue necrosis (a-c), fibrosis (d-f) and nerve body atrophy (axonal loss) (G-I) for each region along the renal artery at 7, 28 and 180 days post radiofrequency renal denervation: Necrosis in the ablated region of the artery was less observeable at 28 days than at 7 days and was not present at 180-days. Fibrosis was apparent at all three time points, but was generally confined to the ablated regions. Axonal loss was present within and beyond the ablated region at all three time points, indicating lack of functional nerve recovery. Gray shaded regions indicate tissue slices located approximately in the ablated region of the vessel, straw colored indicated samples acquired distal to the ablation site. More regions were sampled at 180-days as the model was updated to include branch ablation.

with late arriving renal nerves that converge distally with the main renal artery. Other fibers extending from the ganglionic masses innervate other abdominal and pelvic organs. This complex anatomy risks unpredictable or incomplete nerve destruction following catheter based RDN if energy deliveries are limited to the main renal artery with RF, which, given that no method exists to confirm denervation, might partly explain some prior treatment failures with earlier techniques and technologies in this space.

Limitations

Our analysis has important limitations. Studies were performed in normotensive pigs. However, this model choice is appropriate since the goal was to assess nerve destruction and not BP reduction. Similar to a previous investigation [18], we demonstrated significant reductions in renal cortical NE content and cortical axon density following RF RDN. Also, no physiological test of nerve functionality was performed. However, the observed anatomic changes clearly suggested that functional recovery of once-damaged nerves
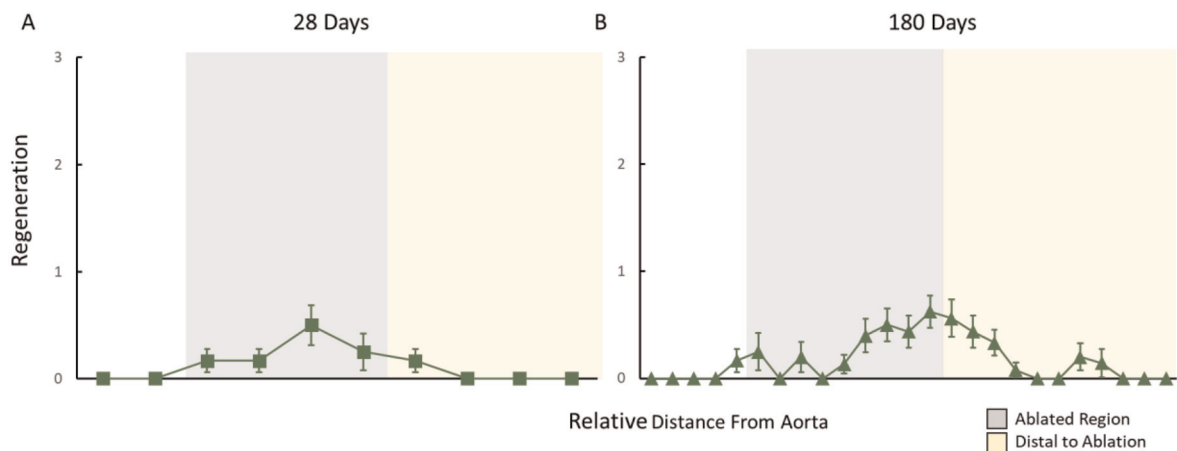

FIGURE 7 Nerve regeneration postradiofrequency renal denervation. Mean nerve regeneration score along the renal artery at 28 and 180-days post radiofrequency renal denervation (scale 0–3). The limited observed neurotamous regeneration was chaotic, with no evidence of functional axonal body formation. Regeneration was not apparent in any samples at 7 days post radiofrequency renal denervation. Regeneration was not consistently evident beyond the approximate ablation region (grey region).

was improbable due to distal axonal loss. Likewise, nerve functionality tests may not be specific since they might inappropriate over-stimulate residual undamaged and potentially hyper-functional nerves. RF RDN was performed in the main renal artery in two groups (7 and 28 days) and also in the primary arterial branches in one group (180 days). However, our analysis focused on the potential for recovery of damaged nerves only. Results from the 180 day main plus branch treated group showed similar results of fibrosis and regeneration confined to the ablation area with downstream axonal destruction. The maximal duration of analysis was limited to 180 days and thus it is possible that longer term follow up may have led to evidence of greater nerve regrowth. However, the sustained axonal loss observed downstream from the site of ablation (Fig. 6), coupled with the confinement of the anatomical regrowth to the ablated region (Fig. 7) severely limits the probability of functional recovery at a later timepoint. In addition, sustained fibrosis in the ablated region (Fig. 6) may physically impede distal proliferation of Schwann cells and neuronal axons. Finally, the present results obtained using RF denervation may not be extrapolated to other forms of renal nerve ablation such as ultrasonic energy [30] or neurotoxin injection [31] since these might differentially effect post ablation nerve regrowth.

Perspective

We found no evidence of functional nerve regrowth, which requires coherent nerve architecture that is no longer present after RF ablation in unmyelinated renal sympathetic nerves. Residual Schwann cells produce chaotic nonmyelinated nerve tissue around the ablation site, but downstream axonal destruction and nerve body axonal loss at 180 days postdenervation makes functional recovery of successfully denervated nerves unlikely. Whether residual nerve function increases in undamaged nerves is unknown. Overall, these results may explain sustained population BP reductions observed in large, real-world registries from human RF RDN procedures. Safe, maximal destruction of renal sympathetic nerves should remain the goal of RDN, as doing so is likely to produce long-term reductions in renal sympathetic nerve activity.

ACKNOWLEDGEMENTS

Conflicts of interest

REFERENCES

1. Mills KT, Stefanescu A, He J. The global epidemiology of hypertension. *Nat Rev Nephrol* 2020; 16:223–237.
2. Kandzari DE, Bohm M, Mahfoud F, Townsend RR, Weber MA, Pocock S, *et al.* Effect of renal denervation on blood pressure in the presence of antihypertensive drugs: 6-month efficacy and safety results from the SPYRAL HTN-ON MED proof-of-concept randomised trial. *Lancet* 2018; 391:2346–2355.
3. Bohm M, Kario K, Kandzari DE, Mahfoud F, Weber MA, Schmieder RE, *et al.* Efficacy of catheter-based renal denervation in the absence of antihypertensive medications (SPYRAL HTN-OFF MED Pivotal): a multicentre, randomised, sham-controlled trial. *Lancet* 2020; 395:1444–1451.
4. Azizi M, Pereira H, Hamdidouche I, Gosse P, Monge M, Bobrie G, *et al.* Adherence to antihypertensive treatment and the blood pressure-lowering effects of renal denervation in the Renal Denervation for Hypertension (DENERHTN) Trial. *Circulation* 2016; 134:847–857.
5. Azizi M, Sanghvi K, Saxena M, Gosse P, Reilly JP, Levy T, *et al.* Ultrasound renal denervation for hypertension resistant to a triple medication pill (RADIANCE-HTN TRIO): a randomised, multicentre, single-blind, sham-controlled trial. *Lancet* 2021; 397:2476–2486.
6. Mahfoud F, Bohm M, Schmieder R, Narkiewicz K, Ewen S, Ruilope L, *et al.* Effects of renal denervation on kidney function and long-term outcomes: 3-year follow-up from the Global SYMPLICITY Registry. *Eur Heart J* 2019; 40:3474–3482.
7. Volz S, Spaak J, Elf J, Jagren C, Lundin C, Stenborg A, *et al.* Renal sympathetic denervation in Sweden: a report from the Swedish registry for renal denervation. *J Hypertens* 2018; 36:151–158.
8. Mahfoud F, Mancia G, Schmieder R, Narkiewicz K, Ruilope L, Schlaich M, *et al.* Renal denervation in high-risk patients with hypertension. *J Am Coll Cardiol* 2020; 75:2879–2888.
9. Hering D, Lambert EA, Marusic P, Walton AS, Krum H, Lambert GW, *et al.* Substantial reduction in single sympathetic nerve firing after renal denervation in patients with resistant hypertension. *Hypertension* 2013; 61:457–464.
10. Seravalle G, D'Arrigo G, Tripepi G, Mallamaci F, Brambilla G, Mancia G, *et al.* Sympathetic nerve traffic and blood pressure changes after bilateral renal denervation in resistant hypertension: a time-integrated analysis. *Nephrol Dial Transplant* 2017; 32:1351–1356.
11. Krum H, Schlaich M, Whitbourn R, Sobotka PA, Sadowski J, Bartus K, *et al.* Catheter-based renal sympathetic denervation for resistant hypertension: a multicentre safety and proof-of-principle cohort study. *Lancet* 2009; 373:1275–1281.

12. Mulder J, Hokfelt T, Knuepfer MM, Kopp UC. Renal sensory and sympathetic nerves reinnervate the kidney in a similar time-dependent fashion after renal denervation in rats. *Am J Physiol Regul Integr Comp Physiol* 2013; 304:R675–R682.

13. Booth LC, Nishi EE, Yao ST, Ramchandra R, Lambert GW, Schlaich MP, May CN. Reinnervation of renal afferent and efferent nerves at 5.5 and 11 months after catheter-based radiofrequency renal denervation in sheep. *Hypertension* 2015; 65:393–400.

14. Singh RR, McArdle ZM, Iudica M, Easton LK, Booth LC, May CN, *et al*. Sustained decrease in blood pressure and reduced anatomical and functional reinnervation of renal nerves in hypertensive sheep 30 months after catheter-based renal denervation. *Hypertension* 2019; 73:718–727.

15. Rousselle SD, Brants IK, Sakaoka A, Hubbard B, Jackson ND, Wicks JR, *et al*. Neuromatous regeneration as a nerve response after catheter-based renal denervation therapy in a large animal model: immunohistochemical study. *Circ Cardiovasc Interv* 2015; 8:e002293.

16. Li S, Hildreth CM, Rahman AA, Barton SA, Wyse BF, Lim CK, *et al*. Renal denervation does not affect hypertension or the renin-angiotensin system in a rodent model of juvenile-onset polycystic kidney disease: clinical implications. *Sci Rep* 2021; 11:14286.

17. Foss JD, Wainford RD, Engeland WC, Fink GD, Osborn JW. A novel method of selective ablation of afferent renal nerves by periaxonal application of capsaicin. *Am J Physiol Regul Integr Comp Physiol* 2015; 308:R112–R122.

18. Mahfoud F, Tunev S, Ewen S, Cremers B, Ruwart J, Schulz-Jander D, *et al*. Impact of lesion placement on efficacy and safety of catheter-based radiofrequency renal denervation. *J Am Coll Cardiol* 2015; 66:1766–1775.

19. Sakakura K, Tunev S, Yahagi K, O'Brien AJ, Ladich E, Kolodgie FD, *et al*. Comparison of histopathologic analysis following renal sympathetic denervation over multiple time points. *Circ Cardiovasc Interv* 2015; 8:e001813.

20. Garcia-Touchard A, Maranillo E, Mompeo B, Sanudo JR. Microdissection of the human renal nervous system: implications for performing renal denervation procedures. *Hypertension* 2020; 76:1240–1246.

21. Sakakura K, Ladich E, Cheng Q, Otsuka F, Yahagi K, Fowler DR, *et al*. Anatomic assessment of sympathetic peri-arterial renal nerves in man. *J Am Coll Cardiol* 2014; 64:635–643.

22. Kline RL, Mercer PF. Functional reinnervation and development of supersensitivity to NE after renal denervation in rats. *Am J Physiol* 1980; 238:R353–R358.

23. Rodionova K, Fiedler C, Guenther F, Grouzmann E, Neuhuber W, Fischer MJ, *et al*. Complex reinnervation pattern after unilateral renal denervation in rats. *Am J Physiol Regul Integr Comp Physiol* 2016; 310:R806–R818.

24. Nomura G, Kurosaki M, Takabatake T, Kibe Y, Takeuchi J. Reinnervation and renin release after unilateral renal denervation in the dog. *J Appl Physiol* 1972; 33:649–655.

25. Shannon JL, Headland R, MacIver AG, Ferryman SR, Barber PC, Howie AJ. Studies on the innervation of human renal allografts. *J Pathol* 1998; 186:109–115.

26. Mauriello A, Rovella V, Borri F, Anemona L, Giannini E, Giacobbi E, *et al*. Hypertension in kidney transplantation is associated with an early renal nerve sprouting. *Nephrol Dial Transplant* 2017; 32:1053–1060.

27. Hansen JM, Abildgaard U, Fogh-Andersen N, Kanstrup IL, Bratholm P, Plum I, Strandgaard S. The transplanted human kidney does not achieve functional reinnervation. *Clin Sci (Lond)* 1994; 87:13–20.

28. Stouffer GA, Dibona GF, Patel A, Kaul P, Hinderliter AL. Catheter-based renal denervation in the treatment of resistant hypertension. *J Mol Cell Cardiol* 2013; 62:18–23.

29. Mompeo B, Maranillo E, Garcia-Touchard A, Larkin T, Sanudo J. The gross anatomy of the renal sympathetic nerves revisited. *Clin Anat* 2016; 29:660–664.

30. Sakakura K, Roth A, Ladich E, Shen K, Coleman L, Joner M, Virmani R. Controlled circumferential renal sympathetic denervation with preservation of the renal arterial wall using intraluminal ultrasound: a next-generation approach for treating sympathetic overactivity. *EuroIntervention* 2015; 10:1230–1238.

31. Fischell TA, Vega F, Raju N, Johnson ET, Kent DJ, Ragland RR, *et al*. Ethanol-mediated perivascular renal sympathetic denervation: preclinical validation of safety and efficacy in a porcine model. *EuroIntervention* 2013; 9:140–147.